

# Radial Basis Function Collocation Models for Water Wave Propagation over a Submerged Breakwater

Yavuz Tokmak<sup>‡</sup>

Civil Engineering Department, Faculty of Engineering and Architecture, İstanbul Gelişim University, Avcılar, 34310, İstanbul, Turkey

(ytokmak@gelisim.edu.tr)

<sup>‡</sup>Corresponding Author; Yavuz Tokmak, Cihangir Mah. Şehit Piyade Onbaşı Murat Şengöz Sok. No:8 Avcılar/ İstanbul, Tel: +90 212 422 7000,

Fax: +90 212 422 7401, ytokmak@gelisim.edu.tr

*Received: 24.07.2018 Accepted: 30.07.2018*

**Abstract-** In this study, two different numerical models are developed using the radial basis function collocation method (RBFCM) for the waves propagating over variable bathymetry. For the verification and validation of the models, submerged breakwater test, present in the literature, is used. One of the models is based on the Navier-Stokes equations where the fluid is assumed to be viscous, incompressible and is of constant density. Also, it is assumed that the flow is unsteady and the turbulent effects are neglected. And for the other model, it is assumed that the fluid is inviscid, incompressible and is of constant density while the flow is assumed to be unsteady and irrotational. On the surface, fully nonlinear forms of the free surface boundary conditions are implemented using the semi-Lagrangian approach. Multiquadric radial basis functions (MQRBF) are used for the approximation of the unknown parameters. Since each of the models requires the solution of an elliptic boundary value problem, extra collocation centers are defined outside the problem domain in the neighborhood of the boundary centers to define both the boundary condition and the governing equation at a boundary center for better accuracy and stability. It is observed that the results of the both models are in agreement with the laboratory test results.

**Keywords** Water wave propagation, radial basis function collocation, numerical modelling, Navier-Stokes equations, Laplace Equation, submerged breakwater.

## 1. Introduction

First generation water wave propagation models are purely mathematical as the only tool was the mathematical theory in the time they were developed. Therefore the solutions lie within the boundaries of the analytical methods and are limited to the manual efforts as the analytical progress in the topic have ended up with the number of terms included from a perturbation series of the parameters. After the Airy [1] linear wave model, nonlinear Stokes [2] wave models were introduced. These two models are applicable to limited range of water depths especially they fail to give good estimates in shallow water. The most recent effort is due to Fenton [3] in which the fifth order Stokes waves are derived to obtain better results in shallow water. The earliest numerical wave propagation model is developed by Chappellear [4] and Dean [5] where they used the stream function equation as the governing equation and the series

expansion definition of the stream function was required to satisfy the dynamic free surface boundary condition (DFSBC) in the least square sense. Dean [5] showed that stream function solutions can be obtained over the entire depth of water. These models are mainly for horizontal bottoms and the solutions are obtained on a 2D vertical plane.

On the other hand, wave models like cnoidal, solitary, Boussinesq, nonlinear shallow water wave model have come into existence to get better estimates in shallow water. Mei and LeMéhauté [6] and Peregrine [7] were the first generation of Boussinesq wave models. In Madsen and Schäffer [8], Gobbi et al. [9], Madsen et al. [10] efforts have been made to extend the validity of Boussinesq wave models for deeper regions. Except some limited solutions, shallow water wave models are numerical and they are depth

averaged models where the solutions are obtained on a horizontal plane and the bottom can vary.

In parallel to the advancements in computer systems, fully nonlinear irrotational wave models have also been developed where the vertical variation of the wave parameter, namely the velocity potential, is possible. In these models due to Romate [11], Broeze [12], Li and Fleming [13] fully nonlinear forms of the free surface boundary conditions were used and the governing equation is the Laplace equation for the velocity potential where the assumption of irrotationality allowed the utilization of the potential theory.

Apart from the potential theory based models introduced until this point, Navier-Stokes wave models have been developed without restricting the flow to be irrotational and any depth limitations. One of the main difficulties in the Navier-Stokes equations is the pressure field which is not expressed explicitly and along with the momentum equations one other independent equation is the continuity which is expressed in terms of the velocity gradients. Therefore, several techniques have been developed to obtain an independent equation of the pressure. For this purpose, Chorin [14] used the projection method to obtain Poisson equation of the pressure field. Several other approaches to the problem can be found in texts Ferziger and Perić [15], Cebeci et al. [16] and Versteeg and Malalasekera [17].

Another issue in the Navier-Stokes models is the turbulent characteristics of the flow that arise due to boundary irregularities or complex flow regions like the wave breaking zone. For the models estimating the wave energy dissipation due to turbulence one method is that the mean flow and the turbulent fluctuations are split and the Reynolds Averaged Navier-Stokes (RANS) are simulated along with a transport model that estimates the turbulent boundary layer and variation of viscosity in this layer. Another method is the Large Eddy Simulation (LES) where the Navier-Stokes equations are by filtering out small eddies. Also, in Direct Numerical Simulation Models (DNS) sufficiently fine spatial grids are used to catch small eddies and sufficiently small time steps are used to capture every necessary length scales and fluctuations. DNS models require much more computer resources compared to alternative methods.

Most of the models introduced here have been developed using the finite differences, finite elements, and finite volume methods. Since these methods require regular meshes, the water wave propagation problem where at least the free surface boundary deforms in time is simulated using special treatments like interpolation, extrapolation or coordinate transformation into a regular domain. Also, as some of the waves approach to the shore, the free surface becomes multiple valued at the locations where the waves overturn. Most of the free surface tracking methods and also numerical techniques fail to simulate the situations where complex geometries are involved. Based on the work of Hardy [18] in which radial basis functions were used to interpolate geophysical surfaces, Kansa [19,20] used radial basis functions to solve partial differential equations (PDEs) where the unknown parameter is expressed as a series of radial

basis functions (RBFs) using the radial distances between the centers collocated throughout the problem domain. Applying the governing differential equation and the boundary conditions to the approximate expression of the independent variable of the PDE, unsymmetric system of equations were obtained and the results were highly accurate. For the unsteady problems, the interpolation coefficients were assumed to change in time and the integrations were performed to compute the evolution of the coefficients and thereby the flow parameters. RBFs can have global or local support. Earlier RBF models have been developed using the global support functions. Recently, Fornberg et al. [21], Flyer et al. [22] and Fornberg and Flyer [23] used RBF-Finite Differences (RBF-FD) in which the finite difference weights are obtained using RBFs and the resulting system matrices are sparse and computationally efficient compared to models using RBFs of global support.

In this study two numerical models were developed to estimate the water wave propagation over variable bathymetry. The submerged breakwater setup of Luth et al. [24] and Beji and Battjes [25] is used for the validation and verification of the models. One of these models is based on the potential theory and the governing equation is the Laplace equation for the velocity potential where the flow is assumed to be irrotational. The fluid is assumed to be inviscid for this model. And the other model is based on the Navier-Stokes equations where turbulent effects are neglected by assuming rotational effects the due to the irregular boundaries do not have enough time to alter the flow field. The fluid is inviscid for the Navier-Stokes models so that viscosity term remains in the momentum equations. Also, for both of the models the fluid is incompressible, there are no other external effects on the free surface like the wind and the bottom is fixed and impermeable.

## 2. Problem Definition and Numerical Formulation of the Potential Theory Model

For a domain in two dimensions (2D), velocity field derivable from a potential function  $\phi = \phi(x, z, t)$ , the continuity equation reduces to the Laplace equation.

$$\nabla^2 \phi = 0 \tag{1}$$

where on the bottom  $z = z_b(x)$

$$\frac{\partial \phi}{\partial z} + \frac{\partial \phi}{\partial x} \frac{\partial z_b}{\partial x} = 0 \tag{2}$$

and on the free surface  $z = \eta(x)$ , the kinematical free surface boundary condition (KFSBC) and semi-Lagrangian form of the DFSBC is valid as shown respectively.

$$\frac{\partial \eta}{\partial t} = \frac{\partial \phi}{\partial z} - \frac{\partial \phi}{\partial x} \frac{\partial \eta}{\partial x} \tag{3}$$

$$\frac{\partial \phi}{\partial t} = -g\eta - \frac{1}{2} |\nabla \phi|^2 + \frac{\partial \phi}{\partial z} \frac{\partial \eta}{\partial x} \tag{4}$$

On the influx boundary, wave parameters are known and in the tests they are obtained from the Stream Function Wave

Theory (SFWT). On the radiation boundary sponge layer is used where after some location  $x = x_s$  the sponge layer starts and the DFSBC becomes

$$\frac{\partial \phi}{\partial x} = -g\eta - \frac{1}{2} |\nabla \phi|^2 + \frac{\partial \phi}{\partial x} \frac{\partial \eta}{\partial x} - c_s(x)\phi \quad (5)$$

with a damping term containing a location dependent coefficient. The sponge coefficient is obtained at a location inside the sponge layer as

$$c_s(x) = \frac{1}{e-1} \left( \frac{e^{|x-x_s|}}{L_s} - 1 \right) \quad (6)$$

where  $L_s$  is the length of the sponge layer. Also, at the end of the sponge layer Sommerfeld radiation boundary condition is used.

$$\frac{\partial \phi}{\partial x} + c \frac{\partial \phi}{\partial x} = 0 \quad (7)$$

where the coefficient  $c$  is the phase speed of the wave if the sponge layer were not used. In the case of sponge layer and estimate of  $c$  is used with one of the schemes presented in Miller and Thorpe [26].

For centers located throughout the domain, the velocity potential at a center denoted by located at can be approximately expressed as

$$\phi(\mathbf{x}_i, t) = \sum_{j=1}^N \alpha_j(t) \varphi(|\mathbf{x}_i - \mathbf{x}_j|, \delta) \quad (8)$$

$|\mathbf{x}_i - \mathbf{x}_j| = r_{ij}$  is the Euclidean distance between two centers,  $\alpha_j(t)$  is the interpolation coefficient, is the RBF with a shape parameter  $\delta$ . The shape parameter is an unknown constant to be determined by trial-and-error during the simulations. If the resulting flow parameters are not known, one method is to calibrate the shape parameter for simpler flows and use it for the complex flows. Another method is to inspect the variation of the results whether they converge to a solution after some trials. Although, some of the RBFs present in the literature do not contain such a shape parameter, multiquadric RBF (MQRBF) of Hardy [18] is used in this study and it contains the shape parameter as given below.

$$\varphi(r_{ij}, \delta) = \sqrt{1 + \delta^2 r_{ij}^2} \quad (9)$$

Obtaining the spatial derivatives of the velocity potential is straightforward as the spatial dependency is introduced by the infinitely differentiable MQRBF. Since the problem is unsteady, integration in time is performed using the sixth order Adams-Bashforth-Moulton predictor and corrector method. Therefore coupling the boundary value problem with the time integrator, the numerical method basically can be expressed as the computation of a boundary value problem followed by the procedure of updating the parameters for the boundary conditions at an instant and performing this at each time step until the final time is reached.

Further modification to the boundary value problem is made by collocating extra centers just outside the domain one for each of the boundary centers. Thereby, the number of independent equations can be used is increased by the number of the boundary centers. This way it is possible to use the governing equation at each of the boundary centers along with the boundary conditions. More detail on the so called PDE collocation on the boundary technique is found in Fedoseyev et al. [27].

### 3. Problem Definition and Numerical Formulation of the Navier Stokes Model

The Navier-Stokes Equations in 2D vertical domain is composed of the momentum equations in the horizontal ( $x$ ) and the vertical ( $z$ ) and the continuity equation as follows.

$$\frac{\partial u}{\partial t} + u \frac{\partial u}{\partial x} + w \frac{\partial u}{\partial z} = -\frac{\partial p}{\partial x} - g \frac{\partial \eta}{\partial x} + \nu \nabla^2 u \quad (10)$$

$$\frac{\partial w}{\partial t} + u \frac{\partial w}{\partial x} + w \frac{\partial w}{\partial z} = -\frac{\partial p}{\partial z} + \nu \nabla^2 w \quad (11)$$

$$\frac{\partial u}{\partial x} + \frac{\partial w}{\partial z} = 0 \quad (12)$$

where  $u$  and  $w$  are the velocity components along the horizontal and vertical respectively.  $p$  is the dynamic pressure per unit density of water and it is obtained from definition of the total pressure per unit density of water  $p_t$  that can expressed as the sum of the hydrostatic and dynamic pressure components.

$$p_t = g(\eta - z) + p \quad (13)$$

In order to deal with the pressure term appearing in the Eq. 10- 11, Chorin [14] proposed the projection method where the time rate of change of velocity components are explicitly discretized and provisional values for these components are defined using the momentum equations without the pressure terms. Namely, denoting the  $n$ -th time step with superscript  $n$  and provisional values with superscript  $*$ , the provisional values are obtained as such.

$$\frac{u^* - u^n}{\Delta t} + u^n \frac{\partial u^n}{\partial x} + w^n \frac{\partial u^n}{\partial z} = \nu \nabla^2 u^n \quad (14)$$

$$\frac{w^* - w^n}{\Delta t} + u^n \frac{\partial w^n}{\partial x} + w^n \frac{\partial w^n}{\partial z} = \nu \nabla^2 w^n \quad (15)$$

where  $\Delta t$  is the time increment. Once these provisional values are computed as a correction step velocity components for the new time step  $n+1$  are obtained as follows.

$$\frac{u^{n+1} - u^*}{\Delta t} = -\frac{\partial p^{n+1}}{\partial x} - g \frac{\partial \eta^{n+1}}{\partial x} \quad (16)$$

$$\frac{w^{n+1} - w^*}{\Delta t} = -\frac{\partial p^{n+1}}{\partial z} \quad (17)$$

Since this correction step requires the pressure field at the new time step, Eq. (10) is differentiated with respect to  $x$  and Eq. (11) is differentiated with respect to  $z$  and the results are summed by imposing continuity to get the following Poisson equation for the pressure field at the new time step.

$$\nabla^2 p^{n+1} = \frac{1}{\Delta t} \left( \frac{\partial u^*}{\partial x} + \frac{\partial w^*}{\partial z} \right) - g \frac{\partial^2 \eta}{\partial x^2} \quad (18)$$

And it is subjected to the ambient pressure on the free surface  $z = \eta(x)$ , namely

$$p = 0 \quad (19)$$

On the influx boundary dynamic pressure per unit density values corresponding to the stream function wave is used. Bottom boundary condition is derived using the no-flux boundary condition and the velocity field correction equations (16) and (17). Since the component of the velocity field along the normal of the bottom boundary cancels out, following boundary condition is obtained.

$$-\frac{\partial p^{n+1}}{\partial x} + \frac{\partial p^{n+1}}{\partial z} = \left( -g \frac{\partial \eta^n}{\partial x} + \frac{u^*}{\Delta t} \right) \left( -\frac{\partial z_b}{\partial x} \right) + \frac{w^*}{\Delta t} \quad (20)$$

Similarly, the radiation boundary condition can be obtained as follows.

$$\frac{\partial p^{n+1}}{\partial x} = -g \frac{\partial \eta^n}{\partial x} + \frac{u^*}{\Delta t} \quad (21)$$

There is no need to define a sponge type condition for the pressure field since the pressure field is dependent on the velocity field. Therefore, once the velocity field is damped in the sponge layer by using an artificial damping term, the pressure damps accordingly.

Similar to the potential model, the Navier Stokes model involves the integration of the variables and the solution of a boundary value problem at each time step. In this model velocity components and the free surface are integrated and boundary value problem is solved for the dynamic pressure per unit density. Also, sixth order Adams-Bashforth-Moulton predictor and corrector method is used as an integrator method.

Velocity components on the free surface are also computed using the semi-Lagrangian approach. Namely if the KFSBC is rewritten as

$$\frac{\partial \eta}{\partial t} = w_s - u_s \frac{\partial \eta}{\partial x} \quad (22)$$

where  $u_s = u(x, \eta(x), t)$  and  $w_s = w(x, \eta(x), t)$  are the velocity components on the free surface, variation of the velocity components in time with respect to a semi-Lagrangian perspective will become

$$\frac{\partial u_s}{\partial t} = \frac{\partial u}{\partial t} \Big|_{z=\eta} + \frac{\partial u}{\partial z} \frac{\partial \eta}{\partial t} \quad (23)$$

$$\frac{\partial w_s}{\partial t} = \frac{\partial w}{\partial t} \Big|_{z=\eta} + \frac{\partial w}{\partial z} \frac{\partial \eta}{\partial t} \quad (24)$$

In the sponge layer and artificial damping term is added to the momentum equations

$$\frac{\partial u}{\partial t} + u \frac{\partial u}{\partial x} + w \frac{\partial u}{\partial z} = -\frac{\partial p}{\partial x} - g \frac{\partial \eta}{\partial x} + \nu \nabla^2 u - c_s(x)u \quad (25)$$

$$\frac{\partial w}{\partial t} + u \frac{\partial w}{\partial x} + w \frac{\partial w}{\partial z} = -\frac{\partial p}{\partial z} + \nu \nabla^2 w - c_s(x)w \quad (26)$$

where definition of the sponge layer coefficient is identical to the Eq. (6).

For  $N$  centers collocated throughout the domain where  $N_b$  of them are located on the boundaries and  $N_s$  of the are located on the free surface, MQRBF discretization of the velocity components, pressure per unit density and the free surface at the  $i$ -th center are written as

$$u_i(r_{ij}, t) = \sum_{j=1}^N \alpha_j^u(t) \sqrt{1 + \delta^2 r_{ij}^2} \quad (27)$$

$$w_i(r_{ij}, t) = \sum_{j=1}^N \alpha_j^w(t) \sqrt{1 + \delta^2 r_{ij}^2} \quad (28)$$

$$p_i(r_{ij}, t) = \sum_{j=1}^{N+N_b} \alpha_j^p(t) \sqrt{1 + \delta^2 r_{ij}^2} \quad (29)$$

$$\eta_i(r_{ij}, t) = \sum_{j=1}^{N_s} \alpha_j^\eta(t) \sqrt{1 + \delta^2 r_{ij}^2} \quad (30)$$

where  $r_{ij}$  is the Euclidean distance between the  $i$ -th and the  $j$ -th centers. Also, for the velocity components the center set collocated throughout the domain is used, for the pressure field extra centers are collocated for each of the boundary centers outside the domain and for the free surface centers only the centers located on the free surface are used.

#### 4. Test Results and Conclusion

An illustration for the test setup of the submerged break water tests is given in Fig. 1. Water depth is 0.4 m and at 6 m from the input boundary decreases to 0.1 m at the top of the breakwater in 6 m with a slope of 1:20. On the lee side of the breakwater, water depth increases to 0.4 m in 3 m with a slope of 1:10. Wave height of the test wave is  $H=0.02m$  and the wave period is  $T = 2.02s$ . The right propagating test wave is a weakly nonlinear intermediate water wave.

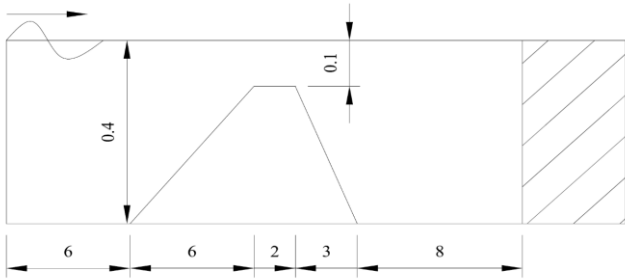


**Fig. 1** Test setup for the submerged breakwater simulations. Variable length sponge layer is shaded. (All dimensions are in meters.)

In accordance with the experimental results of Luth et al. [24], simulation results of the Navier Stokes model and nonlinear potential model at the stations  $x = 5.2, 12.5, 14.5, 17.3$  m are plotted in Fig. 2 to Fig. 5.

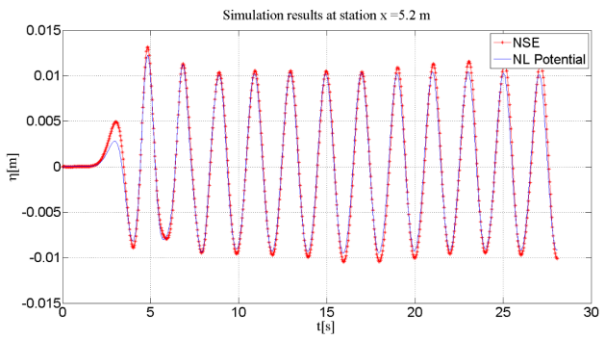


**Fig. 2** Comparison of the Navier Stokes and nonlinear potential model results at station  $x = 5.2$  m

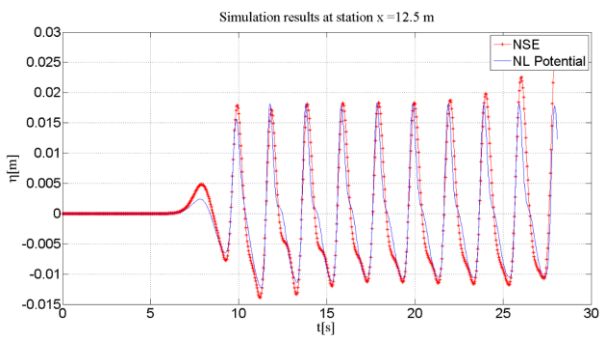


**Fig. 3** Comparison of the Navier Stokes and nonlinear potential model results at station  $x = 12.5$  m

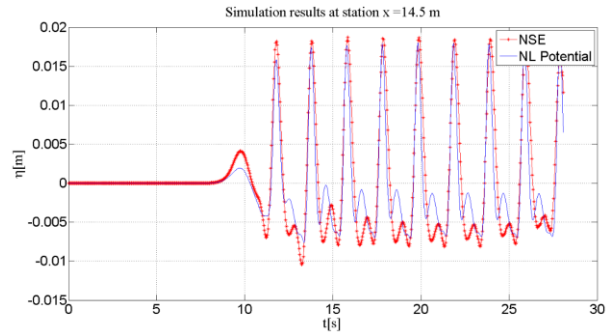


**Fig. 4** Comparison of the Navier Stokes and nonlinear potential model results at station  $x = 14.5$  m

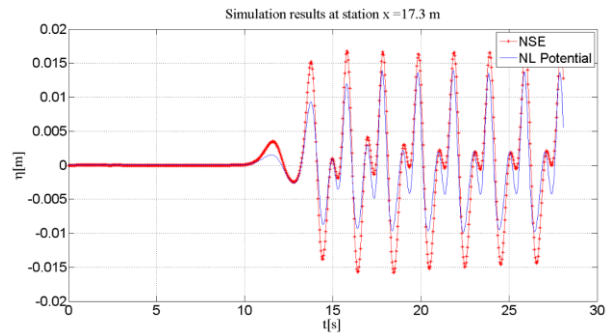


**Fig. 5** Comparison of the Navier Stokes and nonlinear potential model results at station  $x = 17.3$  m

In Fig. 6 to Fig. 9 model results are plotted with the experimental results at the stations  $x = 5.2, 12.5, 14.5, 17.3$  m. These results are extracted from the simulation results at a time later than the beginning of the simulations by visual inspection.

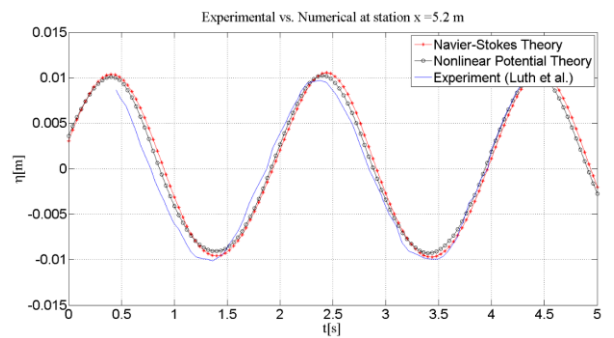


**Fig. 6** Comparison of the numerical model results with the experiment results at station  $x = 5.2$  m

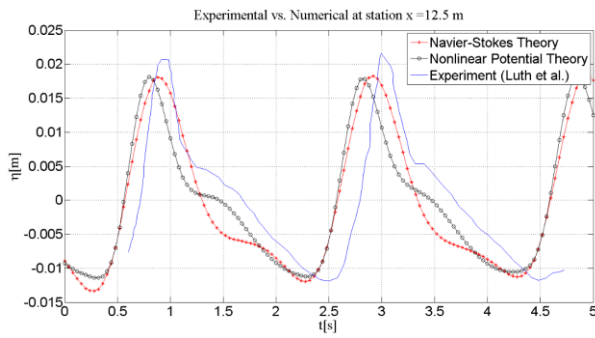


**Fig. 7** Comparison of the numerical model results with the experiment results at station  $x = 12.5$  m

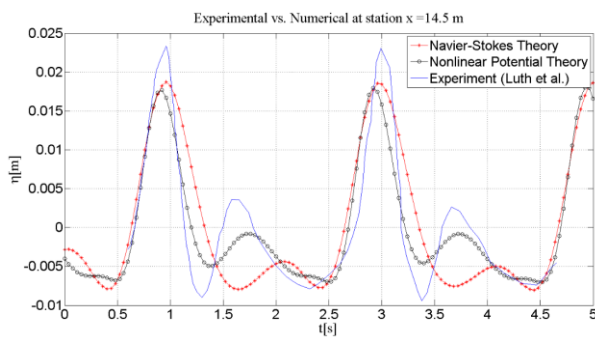


**Fig. 8** Comparison of the numerical model results with the experiment results at station  $x = 14.5$  m

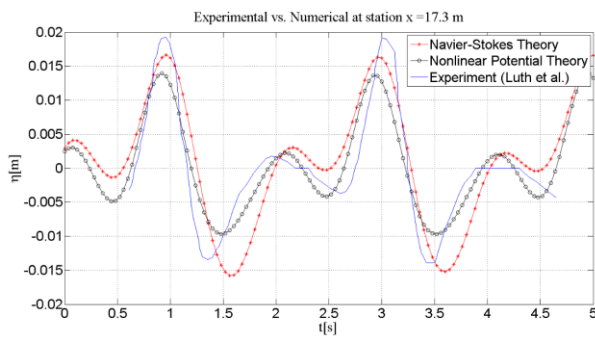


**Fig. 9** Comparison of the numerical model results with the experiment results at station  $x = 17.3$  m

The main difference in the results is caused by the reflection from the radiation boundary which is a sponge layer in the numerical models and a sloping beach in the experiment. As apparent from the figures results are in better agreement at the front of the break water, namely at the station  $x = 5.2$  and  $12.5$  m. On top of the breakwater higher harmonics and higher amplitudes can be observed. The potential theory model results is closer to experiment results compared to those of the Navier Stokes model. On the other hand, at the lee of the breakwater Navier Stokes results are closer to the experiment results compared to those of the potential theory model.

It can be concluded that the RBF collocation method can be used for modeling water wave propagation models. For problems like the free surface flow where the problem domain deforms in time, applying RBFs is easier and higher accuracy can be obtained compared to methods requiring fixed meshes. There is no need to employ some other method to track for the free surface since the RBF centers moves with the free surface.

Extending the applicability of RBF models are also easier, for example including the transverse direction as the third dimension can simply be implemented by replacing the 2D RBFs with 3D versions in the discrete forms of the parameters.

Coupling this model with a transport model and account for turbulent dissipation from the bottom boundary is also straightforward as long as the viscosities and the thickness of the boundary is determined.

## References

- [1] G. Airy, Tides and Waves, London:Encyclopedia Metropolitana, 1845, Tom. V, pp.241-396.
- [2] G. Stokes, "On the Theory of Oscillatory Waves", Trans. Camb. Philos. Soc., Vol. 8, pp. 441-455, 1847.
- [3] J.D. Fenton, "A Fifth-Order Stokes Theory for Steady Waves", ASCE Jour. Waterw., Port, Coastal and Ocean Engr., Vol. 111, pp. 216-234, 1985.
- [4] J.E. Chappellear, "Direct numerical calculation of wave properties", J. Geophys. Res., Vol. 66(2), pp. 501-508, 1961.
- [5] R. Dean, "Stream Function Representation of Nonlinear Ocean Waves", J. Geophys. Res., Vol. 70, pp. 4561-4571, 1965
- [6] C.C. Mei and B. LeMéhauté, "Note on the Equations of Long Waves Over an Uneven Bottom", J. of Geophysical Res., Vol.72, No. 2, pp. 393-400, 1966.
- [7] J. Peregrine, "Long waves on a beach", J. Fluid Mech., Vol.27, No. 4, pp. 815-827, 1967.
- [8] P.A. Madsen and H.A. Schäffer, "Higher-order Boussinesq-type Equations for Surface Gravity Waves – Derivations and Analysis", Phil. Trans. R. Soc. Lond., Seri A, Vol. 356, pp. 1-59, 1998.
- [9] M.F. Gobbi, J.T. Kirby, G. Wei, "A Fully Nonlinear Boussinesq Model for Surface Waves. Part 2 Extension to  $O(kh)^4$ ", J. Fluid Mech., Vol.405, pp. 181-210, 2000.
- [10] Madsen, P.A., Bingham, H.B., Liu, H. (2002). A new Boussinesq method for fully nonlinear waves from shallow to deep water. J. Numer. Meth. Fluids, Vol. 462, pp. 1-30, 2002.
- [11] J.E. Romate, The numerical simulation of nonlinear gravity waves in three dimensions using a higher order panel method, Ph.D. Thesis, Delft Hydraulics, 1989.

- [12] M. Broeze, 1993, Numerical modeling of nonlinear free surface waves with a 3D panel method, Ph. D. Thesis, University of Twente, 1993.
- [13] B. Li, and C.A. Fleming, C.A., "A three dimensional multigrid model for fully nonlinear water waves", Coastal Engineering, Vol. 30, pp. 235-258, 1997.
- [14] A.J. Chorin, "Numerical Solution of Navier Stokes Equations", Math. Comp., Vol. 22, 745-762, 1968.
- [15] J.H. Ferziger and M. Peric, Computational Methods for Fluid Dynamics, Berlin Heidelberg New York: Springer Verlag, 2002.
- [16] T. Cebeci, J.P. Shao, F. Kafyeke, E. Laurendeau, E., Computational Fluid Dynamics For Engineers, Long Beach:Horizons Publishing, 2005.
- [17] H.K. Versteeg, W. Malalasekera, An Introduction to Computational Fluid Dynamics, 2nd ed., Essex:Pearson Education Limited, 2007.
- [18] R.L. Hardy, "Multiquadric equations of topography and other irregular surfaces", Journal of Geophysical Research, Vol. 76(26), pp. 1905-1915, 1971.
- [19] E.J. Kansa, E.J. "Multiquadrics - A Scattered Data Approximation Scheme with Applications to Computational Fluid Dynamics-I Surface Approximations and Partial Derivative Estimates", Computers and Mathematics with Applications, Vol. 19, No. 8/9, pp. 127-145, 1990.
- [20] E.J. Kansa, "Multiquadrics- A Scattered Data Approximation Scheme with Applications to Computational Fluid Dynamics-II Solutions to Parabolic, Hyperbolic and Elliptic Partial Differential Equations", Computers and Mathematics with Applications, Vol. 19, No. 8/9, pp. 147-161, 1990.
- [21] B. Fornberg, E. Lehto, C. Powell, "Stable Calculation of Gaussian-based RBF-FD stencils", Comput. Math. Appl., Vol. 65(4), pp. 627-637, 2013.
- [22] N. Flyer, G.B. Wright, B. Fornberg, B., Radial Basis Function-Generated Finite Differences: A Mesh-Free Method for Computational Geosciences, Handbook of Geomatics: Second Edition, pp. 2635-2669, 2018.
- [23] B. Fornberg, and N. Flyer, A Primer on Radial Basis Functions with Applications to the Geosciences, E-book, Society for Industrial and Applied Mathematics, 2015.
- [24] H. Luth, G. Klopman, and N. Kitou, 1994, Projects 13G: Kinematics of waves breaking partially on an offshore bar: LVD measurements for waves without a net onshore current., Technical Report H1573, Tech. rep., Delft Hydraulics, 1994.
- [25] S. Beji, J.A. Battjes, "Experimental investigation of wave propagation over a bar", Coastal Engineering, Vol.19, pp. 151-162, 1993.
- [26] M.J. Miller and A.J. Thorpe, "Radiation conditions for the lateral boundaries of limited-area numerical models", Quarterly J. Royal Meteorological Society, Vol. 107, pp. 615-628, 1981.
- [27] A.L. Fedoseyev, M.J. Friedman, E.J. Kansa, 2002, "Improved multiquadric method for elliptic partial differential equations via PDE collocation on the boundary", Comput. Math. Appl., Vol. 43(3-5), pp. 439-455, 2002.